Eur. Phys. J. D **10**, 33–38 (2000)

THE EUROPEAN PHYSICAL JOURNAL D

EDP Sciences
© Società Italiana di Fisica
Springer-Verlag 2000

Frequency measurement, isotope shift and hyperfine structure of the $4d^95s^2\ ^2D_{5/2} \rightarrow 4d^{10}6p\ ^2P_{3/2}$ transition in atomic silver

S. Guérandel, T. Badr, M.D. Plimmer[a], P. Juncar, and M.E. Himbert

BNM-INM, Conservatoire National des Arts et Métiers, 292 rue Saint-Martin, 75003 Paris, France

Received 16 July 1999 and Received in final form 7 October 1999

Abstract. The frequency of the centroid of the transition $4d^95s^2\ ^2D_{5/2} \rightarrow 4d^{10}6p\ ^2P_{3/2}$ in Ag I has been determined by laser spectroscopy of a collimated metastable thermal atomic beam. We find $\nu =$ 547 376 388(60) MHz. The isotope shift $\nu(^{109}\mathrm{Ag}) - \nu(^{107}\mathrm{Ag}) = -982.6(5.4)$ MHz. For the magnetic hyperfine structure constant of the $4d^{10}6p\ ^2P_{3/2}$ state, assuming IJ coupling, we find, $A(^{107}\mathrm{Ag}) = -8.4(6)$ MHz and $A(^{109}\mathrm{Ag}) = -10.2(6)$ MHz.

PACS. 32.10.Fn Fine and hyperfine structure – 32.30.Jc Visible and ultraviolet spectra

1 Introduction

The spectrum of the silver atom has been studied by optical spectroscopy for more than 50 years [1]. Most of this work has been performed by analysing the emission spectra of discharge lamps, while measurements by laser spectroscopy have been confined to transitions from the ground state, in particular the D-lines at $\lambda = 328$ nm and 338 nm [2,3]. A fair amount of atomic structure calculation has been carried out on the alkali-like configurations $4d^{10}nl$ [4]. In 1976, the very narrow two-photon transition $4d^{10}5s\ ^2S_{1/2} \rightarrow 4d^95s^2\ ^2D_{5/2}$ in silver [5] was proposed as a candidate for an optical frequency standard by Bender *et al.* [6] (Fig. 1). Since then, developments in laser cooling and trapping of atoms have rekindled interest in this transition [7]. Indeed, a sample of silver atoms has been confined in a magneto-optical trap by the group of Walther in Garching [3] with a view to observing the transition with a narrow linewidth. In our own group, we aim to excite the same transition in a thermal atomic beam as a prelude to work on cold atoms. An indirect measurement of the frequency required to excite the two-photon transition has been carried out by Larkins and Hannaford [8] who measured the emission wavelengths from a hollow-cathode discharge of the line $4d^95s^2\ ^2D_{5/2} \rightarrow 4d^{10}6p\ ^2P_{3/2}$ near 547 nm and that of the $4d^{10}5s\ ^2S_{1/2} \rightarrow 4d^{10}6p\ ^2P_{3/2}$ transition near 206 nm.

One of the principal difficulties is the detection of atoms in the metastable $4d^95s^2\ ^2D_{5/2}$ state. Laser excitation of the $4d^95s^2\ ^2D_{5/2} \rightarrow 4d^{10}6p\ ^2P_{3/2}$ transition is an attractive option since the UV fluorescence at 206 nm resulting from the decay of the $4d^{10}6p\ ^2P_{3/2}$ level is easily observed using a photomultiplier combined with an interference filter.

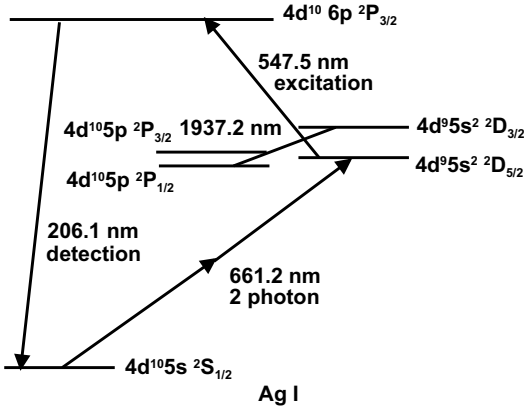

Fig. 1. Partial energy level diagram for Ag I.

In this article we report measurements of the absolute frequency, isotope shift and hyperfine splittings of the line at 547.5 nm performed by laser spectroscopy of a collimated thermal atomic beam. Dinger *et al.* [9] studied this and other transitions in both the stable and radioactive isotopes of silver, using on-line collinear laser spectroscopy of a fast beam. Our work is intended as a cross-check of their results.

2 Experimental set-up

The layout of the experiment is shown in Figure 2. The principal elements are the atomic beam apparatus and the laser sources and frequency calibration system.

[a] e-mail: plimmer@cnam.fr

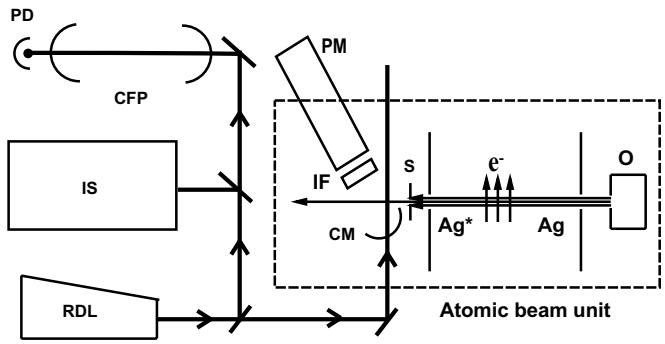

Fig. 2. Experimental set-up. Key: CFP confocal Fabry Perot, CM curved mirror, IF interference filter, IS iodine spectrometer, O oven, PD photodiode, PM photomultiplier, RDL ring dye laser, S slit.

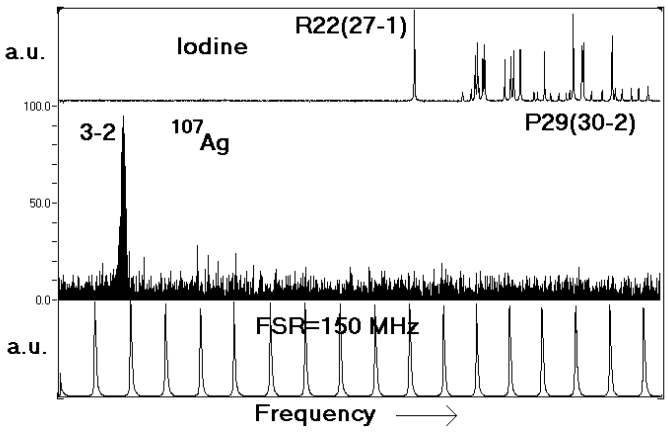

Fig. 3. Scan over the hyperfine component ($F = 3 \rightarrow F' = 2$) of the transition $4d^9 5s^2\ ^2\mathrm{D}_{5/2} \rightarrow 4d^{10}6p\ ^2\mathrm{P}_{3/2}$ for the isotope ^{107}Ag and hyperfine components of the molecular iodine spectrum. The taller iodine peaks correspond to the line R22(27-1), the shorter ones to P29(30-2). The middle vertical axis indicates the number of counts per 0.5 s. Marker fringes from the Fabry Perot cavity are shown below.

2.1 Atomic beam

The atomic beam unit consists of three vacuum chambers evacuated independently by turbo-molecular pumps. Circular apertures (1 cm diameter) guarantee differential pumping of each region. Silver atoms are evaporated at 1200 °C in a thin-walled tantalum oven similar to that described by Benton *et al.* [10]. The atoms pass into a second chamber where a small fraction of them (less than 10^{-6}) is excited to the metastable state *via* electron bombardment. The electron gun is a triode along the same lines as that described by Biraben *et al.* [11]. The mean cathode-grid voltage is about −6 V with the anode maintained at +700 V relative to the grounded grid. The emission current obtained from three filaments in parallel is typically 0.45 mA. Electron bombardment causes a deflection of the metastable beam by 10^{-2} rad and a dispersion by a comparable amount. In a third chamber, the atoms pass through a translatable slit of width 1.5 mm, after which the metastable atoms interact with the laser beam which intersects their trajectory at right angles. The fluorescence at 206 nm is observed with a photomultiplier (Hamamatsu model *R*6834) located outside a sapphire re-entrant window. Light collection efficiency is increased *via* the use of a spherical mirror (diameter 90 mm, radius of curvature 60 mm) situated beneath the interaction region. Scattered laser light at 547 nm as well as radiation from the oven and the filament of the electron gun are reduced by the use of an Aquadag coating of the walls of the third chamber and an interference filter (Omega Optical 210BP10 peak transmission 12.5%, full width at half maximum 10 nm).

2.2 Laser source and frequency calibration

The experiment was performed using a ring dye laser (Coherent model 699-21 with rhodamine 560 dye). Since the transition $4d^9 5s^2\ ^2\mathrm{D}_{5/2} \rightarrow 4d^{10}6p\ ^2\mathrm{P}_{3/2}$ involves the change of two electron orbitals, it is allowed only by configuration mixing and requires a high optical intensity in order to excite it. We use typically a laser power of 300 mW for a beam radius $w = 5$ mm in the interaction region. The laser polarisation is perpendicular to the plane containing the laser and atomic beams. In principle, a greater fluorescence signal would be observed for an orthogonal polarisation. In our own experiment, the insertion of a polarisation rotator caused a loss of optical power and hence no overall gain in signal; all data reported here were taken without it. To measure hyperfine intervals and the isotope shift, the laser frequency was scanned either across the hyperfine structure of a single isotope (a span of about 800 MHz) or else across the entire spectrum of both isotopes (2 GHz). To measure the frequency of the transition, we compared it with that of absorption lines in $^{127}\mathrm{I}_2$ observed using saturated absorption spectroscopy. In this case, the laser frequency was scanned over about 2.5 GHz so as to include a single hyperfine component $F = 3 \rightarrow F' = 2$ in ^{107}Ag and hyperfine components of the transitions R22(27-1) and P29(30-2) of molecular iodine (Fig. 3). Frequency calibration was provided by marker fringes of an invar confocal Fabry Perot cavity (free spectral range 150 MHz) maintained under vacuum at 10^{-2} mbar.

3 Experimental spectra

A spectrum spanning the hyperfine structures of both isotopes is shown in Figure 4. Typical signals of 100–200 counts per second are obtained for the most intense hyperfine component ($F = 3 \rightarrow F' = 2$ in ^{107}Ag) The linewidth of 15 MHz contains contributions from residual Doppler broadening and laser frequency jitter (< 2 MHz) as well as the 3 MHz natural width. The ambient magnetic field, measured with a 3-axis magnetometer (Bartington model MAG-03MC) was less than 0.5 G (5×10^{-5} T), corresponding to a broadening *via* the Zeeman effect of less than 1 MHz. The hyperfine structure of the $6p\ ^2\mathrm{P}_{3/2}$

Table 1. Values (in MHz) of hyperfine splittings and constants and isotope shift $\delta\nu^{107,109}$ obtained from 20 scans using frequency calibration with a FP cavity and an accurately known magnetic hyperfine constant.

calibration method	calculated parameter	value	statistical uncertainty
$A(^2\mathrm{D}_{5/2})(^{107}\mathrm{Ag}) = -126.2818$	$A(^2\mathrm{D}_{5/2})(^{109}\mathrm{Ag})$	-145.12	0.36
	$A(^2\mathrm{P}_{3/2})(^{107}\mathrm{Ag})$	-8.42	0.18
	$A(^2\mathrm{P}_{3/2})(^{109}\mathrm{Ag})$	-10.17	0.20
	$\delta\nu^{107,109}$	-982.49	1.51
$A(^2\mathrm{D}_{5/2})(^{109}\mathrm{Ag}) = -145.1584$	$A(^2\mathrm{D}_{5/2})(^{107}\mathrm{Ag})$	-126.33	0.32
	$A(^2\mathrm{P}_{3/2})(^{107}\mathrm{Ag})$	-8.43	0.19
	$A(^2\mathrm{P}_{3/2})(^{109}\mathrm{Ag})$	-10.16	0.19
	$\delta\nu^{107,109}$	-982.81	1.80

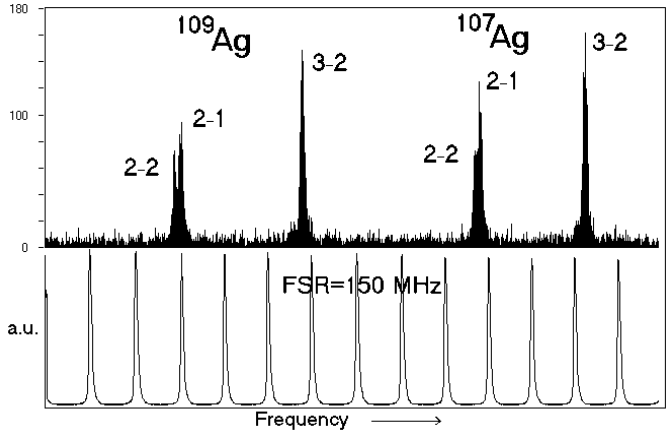

Fig. 4. Scan over the hyperfine structure of the transition $4d^9 5s^2\ ^2\mathrm{D}_{5/2} \rightarrow 4d^{10}6p\ ^2\mathrm{P}_{3/2}$ for the isotopes ^{109}Ag and ^{107}Ag. The upper vertical axis indicates the number of counts per 0.5 s. Marker fringes from the Fabry Perot cavity are shown below.

state is partially resolved in both isotopes. At first sight, the relative intensities of the three hyperfine components ($F = 2 \rightarrow F' = 2$, $F = 2 \rightarrow F' = 1$ and $F = 3 \rightarrow F' = 2$) do not lie in the ratio 1:9:14 as expected from angular momentum considerations. In particular, the intensities of the first two components are similar. Nevertheless, this can be accounted for by wing effects when a best-fit Voigt profile is used to analyse the data. Mixing of hyperfine levels by the Zeeman effect would lead to an increased amplitude of the (2–2) component but should also give rise to an additional resonance (3–1) which we do not observe. However, no saturation effects are observed, the signal size varying linearly with laser power in the range 200–500 mW. Optical pumping effects are believed to be negligible since nearly all atoms excited to the $6p\ ^2\mathrm{P}_{3/2}$ decay to the ground state, the return transition to the metastable state being one-electron forbidden.

4 Data analysis

4.1 Hyperfine structure and isotope shift

Marker fringes generated by the Fabry Perot cavity provided a local frequency reference every 150 MHz. The data files themselves contain values of the voltage used to pilot the laser frequency scan. The unequal voltage intervals between successive FP transmission peaks indicate that the laser scan is non linear. The frequency axis was thus linearised piecemeal by imposing the constraint that the interval between all peaks be constant. Next, the centres of hyperfine components were located by fitting a Voigt profile to the data points using a least squares method (Levenberg-Marquardt). The frequency axis was then calibrated using the hyperfine splitting of the $4d^9 5s^2\ ^2\mathrm{D}_{5/2}$ state in either the isotope ^{107}Ag or ^{109}Ag, both of which have been measured very precisely by radio-frequency spectroscopy [12]. A comparison of the hyperfine splitting of the other isotope predicted from the experimental data provides a test of the accuracy of the linearisation procedure. From these data we extract values for the hyperfine constant A of the $4d^{10}6p\ ^2\mathrm{P}_{3/2}$ state for both isotopes: if the IJ coupling approximation is valid then the splitting is just equal to $2A$. The frequencies of the centroids ν_c of the hyperfine structures of each isotope are calculated by taking moments of their theoretical amplitudes:

$$\nu_\mathrm{c} = \frac{1}{24}(\nu_{22} + 9\nu_{21} + 14\nu_{32}) \qquad (1)$$

where, for example, ν_{22} corresponds to the frequency of the component $F = 2 \rightarrow F' = 2$. The isotope shift $\delta\nu^{107,109} = \nu_\mathrm{c}(^{109}\mathrm{Ag}) - \nu_\mathrm{c}(^{107}\mathrm{Ag})$ is calculated from the frequency difference of the centroids.

The results are presented in Table 1.

4.2 Transition frequency

Using the value of the FSR of the Fabry Perot cavity, the frequency of the absorption component ($F = 3 \rightarrow F' = 2$ in ^{107}Ag) was linked to that of the molecular iodine absorption lines. For the latter, the peak centres were located from a fit to a Lorentzian profile.

4.3 Systematic effects

4.3.1 Zeeman effect of the hyperfine structure

The presence of a magnetic field B in the interaction region gives rise to a shift of the Zeeman sub-levels involved in the transition. The frequency of the transition

$4d^9 5s^2\ {}^2\mathrm{D}_{5/2} F, M_F \rightarrow 4d^{10} 6p\ {}^2\mathrm{P}_{3/2} F', M_{F'}$ is displaced by [13]:

$$\Delta\nu = (\mu_\mathrm{B} B/h)(g_{F'} M_{F'} - g_F M_F) \qquad (2)$$

where μ_B is the Bohr magneton, h the Planck constant and g_F and $g_{F'}$ the values of the Landé factors of the levels involved. These are shown in Table 4. In our experiment the polarisation is almost linear, in which case there is only a broadening but, to first order, no overall shift of the line centres. To place an upper limit on any systematic shift, we consider the case of pure circular polarisation which would excite transitions with $|\Delta M_F| = 1$. In this case, the frequency of the Zeeman component $(F = 2, M_F = 2 \rightarrow F' = 1, M_{F'} = 1)$ is shifted by about 1.6 MHz/G, that of $(F = 2, M_F = 2 \rightarrow F' = 2, M_{F'} = 1)$ by 1.1 MHz/G and $(F = 3, M_F = 3 \rightarrow F' = 2, M_{F'} = 2)$ by 1.4 MHz/G. The measured hyperfine splitting of the state $4d^{10} 6p\ {}^2\mathrm{P}_{3/2}$ would be altered by at most 0.5 MHz/G and that of $4d^9 5s^2\ {}^2\mathrm{D}_{5/2}$ by 0.3 MHz/G. For $B = 0.5$ G this gives shifts of 0.25 MHz and 0.15 MHz. Since the laser polarisation is essentially linear, the actual shifts are estimated to be much smaller than the values above and hence negligible compared to other sources of uncertainty.

4.3.2 Quadratic Stark effect

In the presence of a static electric field of amplitude $\mathbf{E}$ a level $|n\rangle$ of energy E_n undergoes a displacement

$$\Delta E = \sum_k \frac{|\langle n|e\mathbf{E}\cdot\mathbf{r}|k\rangle|^2}{E_n - E_k} \qquad (3)$$

where e is the electronic charge and E_k the energy of a level $|k\rangle$. An upper limit on this effect can be estimated using a value for the matrix element of ea_0 where a_0 is the Bohr radius and an energy denominator corresponding to a wavelength of 600 nm. In our experiment, the Aquadag coating of the walls surrounding the interaction region helps reduce stray fields. Experiments performed elsewhere have indicated these fields can be as small as 15 mV/cm [11]. A pessimistic value of 1 V/cm would produce a shift of a few kilohertz which is negligible.

4.3.3 First-order Doppler shift

If the angle at which the laser crosses the atomic beam is different from 90° the frequency at which the atom absorbs is shifted by the first-order Doppler effect. Since the displacement is of order 1 MHz/mrad, this is potentially the most serious source of systematic error. In order to overcome this difficulty, for measurements of the absolute frequency of the transition, the trajectory of the laser beam is adjusted to intersect the atomic beam at a slight angle to the perpendicular so as to produce a deliberate shift. The laser beam is then retro-reflected so as to induce a second resonance with an equal but opposite Doppler shift. In this way, for each hyperfine component, two sets of peaks are observed with slightly different frequencies. The average of the two values gives the rest frequency. A fine application of this approach is described in [14].

Table 2. Absolute frequencies (in MHz) of hyperfine components of the transition $4d^9 5s^2\ {}^2\mathrm{D}_{5/2} F \rightarrow 4d^{10} 6p\ {}^2\mathrm{P}_{3/2} F'$. The standard uncertainty of each value is 60 MHz.

Isotope	F	F'	Frequency
^{109}Ag	2	2	547 375 614
^{109}Ag	2	1	547 375 634
^{109}Ag	3	2	547 376 049
^{109}Ag		centroid	547 375 876
^{107}Ag	2	2	547 376 630
^{107}Ag	2	1	547 376 648
^{107}Ag	3	2	547 377 010
^{107}Ag		centroid	547 376 858
^{109}Ag, ^{107}Ag		centroid of both	547 376 385

4.3.4 Non-linearity of the laser frequency scan

Errors due to departures from linearity of the laser frequency scan are revealed by a comparison of measured and predicted hyperfine structure intervals (*cf.* Tab. 2). The discrepancies are of the order 0.15 MHz for intervals of about 400 MHz. This corresponds to 0.40 MHz for the isotope shift (−983 MHz) or 0.45 MHz for the frequency relative to the molecular iodine components.

4.3.5 Other sources of systematic shift

Since measurements on Ag are performed on an atomic beam in a vacuum better than 10^{-6} mbar, collisional shifts are negligible. For the frequencies of the iodine components, temperature corrections are necessary only to obtain absolute accuracies at the few kilohertz level. Light shifts affect the measurement of the $4d^{10} 6p\ {}^2\mathrm{P}_{3/2}$ hyperfine splitting at the level of 100 kHz for the laser intensities employed in our experiment. Individual peaks could not be fitted to this level of accuracy so no systematic study of the laser power dependence of the positions was carried out. The second order Doppler shift is of order 1 kHz and thus totally negligible at the level of accuracy obtained in this experiment.

4.4 Discussion

In Table 3 we present the values of hyperfine data and isotope shift obtained from the ensemble of our data. The uncertainties quoted are the sample standard deviations, compared with which the systematic effects discussed above are negligible.

Table 3. Magnetic hyperfine interaction constants and isotope shift (MHz).

	This work	[9]	[15]	[16]
$A(6^2\mathrm{P}_{3/2})(^{107}\mathrm{Ag})$	−8.4(6)	−5(2)	−9.05(25)	—
$A(6^2\mathrm{P}_{3/2})(^{109}\mathrm{Ag})$	−10.2(6)	−9(2)	—	—
$\delta\nu^{107,109}$	−982.6(5.4)	−976(8)	—	−960(15)

4.4.1 Hyperfine structure

The hyperfine structure of the metastable $4d^9 5s^2\ ^2\mathrm{D}_{5/2}$ state of both isotopes has been determined by Blachman *et al.* [12]. For the $4d^{10}6p\ ^2\mathrm{P}_{3/2}$ state, the hyperfine structure of the isotope ^{107}Ag has been measured by a quantum beat method by Bengtsson *et al.* [15] who found ($A = -9.05(25)$ MHz). Our result of −8.4(6) MHz lies somewhat below their value though the error bars of both measurements overlap. For the isotope ^{109}Ag, if one neglects the small hyperfine anomalies, the combined results of Bengtsson *et al.* and Blachman *et al.* would imply a value $A(6p\ ^2\mathrm{P}_{3/2}) = -10.4(3)$ MHz. Our own result, −10.2(6) MHz, is in good agreement with this number. Our values are also in rough agreement with those obtained by Dinger *et al.* [9] who found $A(^{109}\mathrm{Ag}) = -9(2)$ and $A(^{107}\mathrm{Ag}) = -5(2)$ MHz.

4.4.2 Isotope shift

The isotope shift of the transition at 547 nm was first measured by Rasmussen [16] who deduced a value of −960(15) MHz from a spectrum of two Doppler broadened components observed in emission from a discharge lamp. To check whether the value of Rasmussen was reasonable, Larkins and Hannaford [8] estimated a value of −1010 MHz based on the isotope shift of the $4d^{10}5p\ ^2\mathrm{P}_{1/2} \rightarrow 4d^9 5s^2\ ^2\mathrm{D}_{3/2}$ transition at 1937.2 nm measured by Fischer *et al.* [17] and plausible assumptions concerning the mass and field shift contributions. Our measured value of −982.6(5.4) MHz lies midway between the result of Rasmussen and the estimate by Larkins and Hannaford. Dinger *et al.* [9] obtained a more precise value of −976(8) MHz using collinear laser spectroscopy. We confirm this value to within their error bar.

4.4.3 Transition frequency

The frequencies of all the hyperfine components are presented in Table 4. The uncertainty of 60 MHz comes from the calibration of the iodine lines whose frequencies have been measured by Gerstenkorn and Luc [18,19]. Shifts arising from temperature differences between our iodine cell and that used to produce the Aimé Cotton atlas are below 1 MHz. Other sources of error are negligible at this level. Our value of $\nu = 547\,376\,385(60)$ MHz for the centroid of the transition lies 64 MHz below that of $\nu = 547\,376\,449(60)$ MHz published by Larkins and Hannaford [8] though the error bars of both measurements overlap. Dinger *et al.* [9] published values of the centroids for both ^{109}Ag (547 375 830(60) MHz) and ^{107}Ag (547 375 880(50) MHz). Our results lie within 22 MHz of theirs for ^{109}Ag and within 46 MHz for ^{107}Ag.

Table 4. Landé factors of the hyperfine levels involved in the transition.

Level	g_F
$^2\mathrm{P}_{3/2}\ F' = 1$	4/3
$^2\mathrm{P}_{3/2}\ F' = 2$	5/3
$^2\mathrm{D}_{5/2}\ F = 2$	6/5
$^2\mathrm{D}_{5/2}\ F = 3$	7/5

5 Conclusion

We have performed measurements on the transition $4d^{10}5s^2\ ^2\mathrm{D}_{5/2} \rightarrow 4d^{10}6p\ ^2\mathrm{P}_{3/2}$ in Ag I near $\lambda = 547$ nm using laser spectroscopy of a metastable atomic beam. In particular, we have determined the ^{107}Ag–^{109}Ag isotope shift and hyperfine splittings of the components involved. We believe our measurement of the isotope shift of this transition to be the most accurate performed thus far. Our determinations of the absolute frequencies of the hyperfine components confirm the values obtained by other authors with similar resolution (60 MHz). We have shown that laser induced fluorescence provides one way of detecting a beam of silver atoms in the metastable $4d^{10}5s^2\ ^2\mathrm{D}_{5/2}$ state with a low background. This work should have applications relating to two-photon spectroscopy of the $4d^{10}5s\ ^2\mathrm{S}_{1/2} \rightarrow 4d^9 5s^2\ ^2\mathrm{D}_{5/2}$ transition, as well as to single photon spectroscopy of transitions originating from the metastable $4d^9 5s^2\ ^2\mathrm{D}_{5/2}$ levels of silver.

S.G. and T.B. are grateful to the MENRT for providing research studentships. The authors thank P.E.G. Baird for supplying a reference on curve fitting, G. Huber for an invaluable reference to his own work and J.A.R. Griffith for information on oven design. L.R. Pendrill provided helpful criticism of the manuscript. This work is supported in part by the Bureau National de Métrologie and the Conseil Régional de l'Île de France *via* a contract LUMINA.

References

1. A.G. Shenstone, Phys. Rev. **57**, 894 (1940).
2. J. Dirscherl, H. Walther, Poster Abstract 1H3, *14th International Conference on Atomic Physics*, Boulder, 31 July-5 August 1994.
3. J. Dirscherl, Ph.D. thesis, Ludwig-Maximillians-Universität, Munich, 1995.
4. J. Migdalek, W.E. Baylis, J. Phys. B **11**, L497 (1978).
5. R.H. Garstang, J. Res. Nat. Bur. Stand. Sect. A **68**, 61 (1964).
6. P.L. Bender, J.L. Hall, R.H. Garstang, F.M.J. Pichanick, W.W. Smith, R.L. Barger, J.B. West, Bull. Am. Phys. Soc. **21**, 599 (1976).
7. J.L. Hall, M. Zhu, P. Buch, J. Opt. Soc. Am. B **6**, 2194 (1989).
8. P.L. Larkins, P. Hannaford, Z. Phys. D **32**, 167 (1994).
9. U. Dinger, J. Eberz, G. Huber, R. Menges, R. Kirchner, O. Klepper, T. Kühl, D. Marx, Nucl. Phys. A **503**, 331 (1989).
10. D.M. Benton, J.L. Cooke, J.A.R. Griffith, J. Phys. B **27**, 4365 (1994).
11. F. Biraben, J.C. Garreau, L. Julien, M. Allegrini, Rev. Sci. Instrum. **61**, 1468 (1990).
12. A.G. Blachman, D.A. Landman, A. Lurio, Phys. Rev. **150**, 59 (1966).
13. N.F. Ramsey, *Molecular Beams* (Oxford University Press, 1956).
14. D.J. Berkeland, E.A. Hinds, M.G. Boshier, Phys. Rev. Lett. **75**, 2470 (1995).
15. J. Bengtsson, J. Larsson, S. Svanberg, Phys. Rev. A **42**, 5457 (1990).
16. E. Rasmussen, Det. Kgl. Danske Videnskabernes Selskab., Mathematisk-fysiske. Medd. **18**, 1 (1940).
17. W. Fischer, H. Hühnermann, E. Krüger, Z. Phys. **216**, 136 (1968).
18. S. Gerstenkorn, P. Luc, Atlas du spectre d'absorption de la molécule d'iode, Laboratoire Aimé Cotton, CNRS II, 1978.
19. S. Gerstenkorn, P. Luc, Rev. Phys. Appl. **14**, 791 (1979).